Journal of Solid Mechanics Vol. 10, No. 2 (2018) pp. 249-262

Combination Resonance of Nonlinear Rotating Balanced Shafts Subjected to Periodic Axial Load

M.S. Qaderi , S.A.A. Hosseini *, M. Zamanian

Department of Mechanical Engineering, Faculty of Engineering, Kharazmi University, Tehran, Iran

Received 21 January 2018; accepted 23 March 2018

ABSTRACT

Dynamic behavior of a circular shaft with geometrical nonlinearity and constant spin, subjected to periodic axial load is investigated. The case of parametric combination resonance is studied. Extension of shaft center line is the source of nonlinearity. The shaft has gyroscopic effect and rotary inertia but shear deformation is neglected. The equations of motion are derived by extended Hamilton principle and discretized by Galerkin method. The multiple scales method is applied to the complex form of equation of motion and the system under parametric combination resonance is analyzed. The attention is paid to analyze the effect of various system parameters on the shape of resonance curves and amplitude of system response. Furthermore, the role of external damping on combination resonance of linear and nonlinear systems is discussed. It will be shown that the external damping has different role in linear and nonlinear shaft models. To validate the perturbation results, numerical simulation is used.

Keywords: Rotating shaft; Parametric excitation; Multiple scales method.

1 INTRODUCTION

ROTATING shafts are the most important structures used to transmit power and motion. Thus predicting accurate dynamic behavior of the rotors is essential. Parametric vibration which is due to dependence of system parameters to time is one of the excitation sources that in linear cases can destabilize the system. There are so many reports on parametrically excited linear rotor systems. Chen and Ku [1] studied a Timoshenko model of a rotating shaft in which axial force was exerted at the end of the shaft. They used finite element method to construct the model and applied Bolotin's method to find stability regions. Lee et al [2] investigated a Timoshenko rotating shaft with time dependent spin rate. They showed that governing equation of motion is not in standard form of Mathieu – Hill equation. The boundaries of instability were presented with respect to different parameters. Sheu and Chen [3] proposed a cantilever shaft with concentrated mass. The shear deformation of shaft was included in their work. They used Bolotin's method to fine instable regions of the shaft dynamics. The difference between Bolotin's and Floquet's methods to find stability boundaries of a rotor with gyroscopic effect was studied by Pei [4]. Bartylla [5] in his paper focused on the effect of periodic axial force on non – symmetric rotor and showed that periodic axial force can stabilize the motion. Mailybaev and Seyranian [6] studied a finite degrees of freedom linear rotor with presence of internal and external damping. The rotor had small axial asymmetry. They presented instability region of that system. In another paper, Mailybaev and Korspeter [7] studied the effect of asymmetry in both bearings and rotor on

*Corresponding author. Tel.: +98 26 34569555; Fax: +98 26 34569555.
E-mail address: ali.hosseini@khu.ac.ir (S.A.A. Hosseini).

the stability boundaries of the shaft vibration. The Laval rotor model was considered and internal and external damping were included to derive equation of motion. It is well known that nonlinearity can stabilize the unstable motion and thus true dynamical behavior of a rotor can be obtained by nonlinear analysis. Bolotin [8] investigated principal parametric resonances in rotors with nonlinear effects. Nonlinear vibrations of unsymmetrical rotor system with concentrated mass model have been studied vastly by Yamamoto and coworkers [9–14]. They reported different kinds of nonlinear resonances. Ishida et al [15] investigated forced oscillation of an asymmetrical rotor with nonlinear spring characteristics. They discussed theoretically and experimentally the effects of this type of nonlinearity on unstable motion of the rotor. Furthermore, Ishida et al [16] studied a continuous horizontal asymmetrical shaft was is under gravity influence and had nonlinear spring characteristics. They considered isolated and internal resonances that occur in this system. Shahgholi and Khadem [17] analyzed a continuous unbalanced shaft which has asymmetry in stiffness and rotary inertia. They studied primary resonance of this system and showed that in this case, only forward mode is excited. They presented the effect of various parameters on the shape of resonance curves. Shahgholi et al [18] investigated nonlinear vibration of a rotating shaft with multi rigid disks. They used multiple scales method. Arani et al [19] analyzed two-dimensional electro-mechanical analysis of a composite rotating shaft. The shaft was excited by non-axisymmetric internal pressure and external voltage.

The above survey shows that the secondary resonance in balanced nonlinear continuous rotating shafts under periodic axial force has not been studied. In this paper, the nonlinear dynamic behavior of a slender shaft with circular cross section subjected to periodic axial force is investigated. In the present model, rotary inertia and gyroscopic effect are considered but shear deformation is neglected and the shaft is assumed to be simply supported. The nonlinearity is due to extension of the rotor center line. Free and forced vibration of a circular shaft with this type of nonlinearity have been analyzed before. [20 – 21] Here, the source of excitation is parametric excitation due to periodic axial force and the type of resonance is combination resonance. Equations of motion are derived by extended Hamilton principle and they are discretized by Galerkin method. By the use of multiple scales method, the complex form of equation of motion is analyzed and reduced to four first order differential equations. With the aid of mathematical operations, these four equations are simplified to one equation which is frequency response equation. The effect of various parameters on the shape of resonance curves is investigated. Specifically, the effect of external damping on combination resonance of linear and nonlinear systems is considered. Numerical method is applied to equations of motion to validate the perturbation result and it is shown that the results of two methods are in good agreement.

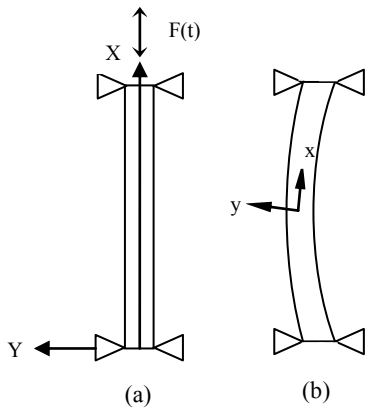

Fig.1
Schematic view of undeformed and deformed shaft with inertial and local coordinate.

2 EQUATIONS OF MOTION

Fig. 1 depicts schematic view of undeformed and deformed rotating shaft. *X–Y–Z* frame is an inertial frame and *x–y–z* attached to the principal axes of the shaft is local coordinate. The equations of motion are described with respect to inertial coordinate system using extended Hamilton principle. $u(x,t)$, $v(x,t)$ and $w(x,t)$ are displacement of a particle in deflected shaft at arbitrary location along *X, Y* and *Z* coordinate, respectively.

In derivation of equations, following assumptions are employed:

1) The shaft is balanced and slender.

2) Rotary inertia and gyroscopic effects are included.
3) Shear deformation and effect of gravity are neglected.
4) The rotating shaft is simply supported.
5) The effect of stretching nonlinearity due to extension of the shaft centerline is considered.
6) External damping is considered.
7) The periodic axial load is exerted at the end of rotating shaft.

As mentioned before, extended Hamilton principle is used to derive equations of motion:

$$\int_{t_1}^{t_2} \delta(T - U)dt + \int_{t_1}^{t_2} \delta W_{nc} dt = 0 \tag{1}$$

where T and U indicate kinetic and potential energies, respectively and W_{nc} is due to non-conservative forces. The kinetic and potential (strain) energies are as follows [20]:

$$T = \frac{1}{2}\int_0^l \left\{\rho A\left(\dot{u}^2 + \dot{v}^2 + \dot{w}^2\right) + I_1\omega_1^2 + I_2\left(\omega_2^2 + \omega_3^2\right)\right\} \tag{2}$$

$$U = \frac{1}{2}\int_0^l \left(A_{11}e^2 + D_{11}\rho_1^2 + D_{22}\rho_2^2 + D_{22}\rho_3^2\right) \tag{3}$$

where

$$I_1 = \int_A \rho\left(y^2 + z^2\right)dA, I_2 = \int_A \rho y^2 dA = \int_A \rho z^2 dA \tag{4}$$

and

$$A_{11} = \int_A EdA,\ D_{11} = \int_A G\left(y^2 + z^2\right)dA,\ D_{22} = \int_A Ey^2 dA = \int_A Ez^2 dA, \tag{5}$$

$\omega_i\ (i = 1-3)$ is angular velocity of the deformed frame, E and G are elasticity and shear modulus respectively and $\rho_i\ (i = 1-3)$ is curvature. e is strain along the centerline axis which is obtained as follows:

$$e = \sqrt{(1+u')^2 + v'^2 + w'^2} - 1 \approx u' + \frac{1}{2}\left(v'^2 + w'^2\right) \tag{6}$$

The boundary conditions are [20]:

$$\begin{aligned} &u(0,t) = 0, u(l,t) = \delta \\ &v(0,t) = w(0,t) = 0, v''(l,t) = w''(l,t) = 0 \end{aligned} \tag{7}$$

where $\delta = \dfrac{Fl}{AE}$ and F is axial load which has static and dynamic parts as indicated below:

$$F = f + P\cos\omega t \tag{8}$$

From the above equations and with regard to details presented in references [20] and [22], the equations of motion in dimensionless form with presence of external damping are obtained:

$$F = f + P\cos\omega t \tag{8}$$

$$\ddot{v} + \mu_e \dot{v} - I_2 \ddot{v}'' - 2I_2 \Omega \dot{w}'' + v^{(iv)} - F v'' - \alpha \left[\int_0^l \left(v'^2 + w'^2 \right) \right] v'' = 0 \tag{9}$$

$$\ddot{w} + \mu_e \dot{w} - I_2 \ddot{w}'' + 2I_2 \Omega \dot{v}'' + w^{(iv)} - F w'' - \alpha \left[\int_0^l \left(v'^2 + w'^2 \right) \right] w'' = 0 \tag{10}$$

where dimensionless parameters are:

$$\bar{x} = \frac{x}{l}, \bar{v} = \frac{vl}{r_0^2}, \bar{w} = \frac{wl}{r_0^2}, r_0^2 = \frac{I}{A}, \tau = \gamma t, \gamma = \sqrt{\frac{EI}{\rho A l^4}}, \bar{\mu}_e = \frac{\mu_e l^2}{\sqrt{\rho A E I}}, \bar{I}_2 = \frac{I_2}{\rho A l^2}, \bar{\Omega} = \frac{\Omega}{\gamma}, \bar{F} = \frac{F l^2}{EI}, \alpha = \frac{A r_0^4}{2 I l^2} \tag{11}$$

Here, r_0 is the radius of gyration of the cross section of the shaft. For simplicity in Eqs. (9) and (10), the over bars have been dropped. To analyze the above equations, Galerkin method is applied to Eqs. (9) and (10). The solution of Eqs. (9) and (10) are assumed in the form:

$$v = v_n(\tau)\phi_n(x), \quad w = w_m(\tau)\phi_m(x) \tag{12}$$

where $v_n(\tau)$ and $w_m(\tau)$ are unknown functions of time τ and mode shape is $\phi_n = \sqrt{2}\sin(n\pi x)$. Substituting (12) into (9) and (10), using Galerkin method for the first mode, the following equation in complex form is obtained:

$$\begin{aligned} &\left(1 + I_2 \pi^2\right) \ddot{Z}(t) + \pi^4 Z(t) - 2I_2 \Omega \pi^2 \dot{Z}(t) i + \mu_e \dot{Z}(t) + \pi^2 f Z(t) + \frac{1}{2}\pi^2 P e^{i\omega t} Z(t) + \frac{1}{2}\pi^2 P e^{-i\omega t} Z(t) \\ &+ \alpha \pi^4 \bar{Z}(t) Z(t)^2 = 0 \end{aligned} \tag{13}$$

where

$$Z = v + iw, \quad \bar{Z} = v - iw \tag{14}$$

3 METHOD OF MULTIPLE SCALES

In this section, multiple scales method [23] is applied to determine a first–order uniform expansion for the solutions of (13). Here, Z and $\bar{Z}$ are expanded in the form:

$$\begin{aligned} Z(t) &= \varepsilon Z_1(T_0, T_2) + \varepsilon^3 Z_3(T_0, T_2), \\ \bar{Z}(t) &= \varepsilon \bar{Z}_1(T_0, T_2) + \varepsilon^3 \bar{Z}_3(T_0, T_2) \end{aligned} \tag{15}$$

where $T_0 = t$ and $T_2 = \varepsilon^2 t$ are fast and slow time scales, respectively and ε is a small dimensionless parameter. In this method, P and external damping are so scaled that their influence are balanced with nonlinearities. Therefore, one may write:

$$P = P\varepsilon^2, \quad \mu_e = \mu_e \varepsilon^2 \tag{16}$$

Time derivatives in terms of T_0 and T_2 are obtained using chain rule:

$$\frac{d}{dt}=D_0+\varepsilon^2 D_2,\quad \frac{d^2}{dt^2}=D_0^2+2\varepsilon^2 D_0 D_2 \tag{17}$$

where $D_n=\dfrac{\partial}{\partial T_n},(n=0,2)$. By substituting Eqs. (15)– (17) Into Eq. (13) and replacing ωt by ωT_0, and equating the coefficients of the same power of ε, the following equations are obtained:

$O(\varepsilon)$:

$$\left(I_2\pi^2+1\right)\left(\frac{\partial^2}{\partial T_0^2}Z_1\left(T_0,T_2\right)\right)-2I_2\Omega\pi^2\left(\frac{\partial}{\partial T_0}Z_1\left(T_0,T_2\right)\right)i+\left(\pi^4+\pi^2 f\right)Z_1\left(T_0,T_2\right)=0 \tag{18}$$

$O(\varepsilon^3)$:

$$\begin{aligned}&\left(1+I_2\pi^2\right)\left(\frac{\partial^2}{\partial T_0^2}Z_3\left(T_0,T_2\right)\right)-2I_2\Omega\pi^2\left(\frac{\partial}{\partial T_0}Z_3\left(T_0,T_2\right)\right)i\\&\left(\pi^4+\pi^2 f\right)Z_3\left(T_0,T_2\right)=2I_2\Omega\pi^2\left(\frac{\partial}{\partial T_2}Z_1\left(T_0,T_2\right)\right)i-\mu_e\left(\frac{\partial}{\partial T_0}Z_1\left(T_0,T_2\right)\right)-\frac{1}{2}\pi^2 PZ_1\left(T_0,T_2\right)e^{-i\omega T_0}-\frac{1}{2}\pi^2 Pe^{i\omega T_0}Z_1\left(T_0,T_2\right)\\&-\left(2+2I_2\pi^2\right)\left(\frac{\partial^2}{\partial T_2\partial T_0}Z_1\left(T_0,T_2\right)\right)-\alpha\pi^4\overline{Z}_1\left(T_0,T_2\right)Z_1\left(T_0,T_2\right)^2\end{aligned} \tag{19}$$

The solution of (18) can be expressed in terms of the linear free vibration modes as:

$$\begin{aligned}Z_1\left(T_0,T_2\right)&=A_1\left(T_2\right)e^{i\beta_1 T_0}+A_2\left(T_2\right)e^{-i\beta_2 T_0}\\\overline{Z}_1\left(T_0,T_2\right)&=\overline{A}_1\left(T_2\right)e^{-i\beta_1 T_0}+\overline{A}_2\left(T_2\right)e^{i\beta_2 T_0}\end{aligned} \tag{20}$$

where β_1 and β_2 are forward and backward linear natural frequencies, respectively. They are computed as:

$$\begin{aligned}\beta_1&=\frac{I_2\Omega\pi^2+\sqrt{I_2^2\Omega^2\pi^4+\pi^6 I_2+\pi^4+\pi^4 fI_2+\pi^2 f}}{I_2\pi^2+1}\\\beta_2&=\frac{-I_2\Omega\pi^2+\sqrt{I_2^2\Omega^2\pi^4+\pi^6 I_2+\pi^4+\pi^4 fI_2+\pi^2 f}}{I_2\pi^2+1}\end{aligned} \tag{21}$$

Coefficients A_1 and A_2 are obtained in the next stage. Substituting (20) into (19) yields:

$$\begin{aligned}&\left(\pi^4+\pi^2 f\right)Z_3\left(T_0,T_2\right)+\left(1+I_2\pi^2\right)\left(\frac{\partial^2}{\partial T_0^2}Z_3\left(T_0,T_2\right)\right)-2I_2\Omega\pi^2\left(\frac{\partial}{\partial T_0}Z_3\left(T_0,T_2\right)\right)i\\&=[\mu_e\beta_1 A_1\left(T_2\right)i+\left(2I_2\Omega\pi^2-2I_2\pi^2\beta_1-2\beta_1\right)\left(\frac{d}{dT_2}A_1\left(T_2\right)\right)i-\alpha\pi^4\overline{A}_1\left(T_2\right)A_1\left(T_2\right)^2\\&-2\alpha\pi^4\overline{A}_2\left(T_2\right)A_1\left(T_2\right)A_2\left(T_2\right)]e^{i\beta_1 T_0}+[\left(2\beta_2+2I_2\pi^2\beta_2+2I_2\Omega\pi^2\right)\left(\frac{d}{dT_2}A_2\left(T_2\right)\right)i+\mu_e\beta_2 A_2\left(T_2\right)i\\&-2\alpha\pi^4\overline{A}_1\left(T_2\right)A_1\left(T_2\right)A_2\left(T_2\right)-\alpha\pi^4\overline{A}_2\left(T_2\right)A_2\left(T_2\right)^2]e^{-i\beta_2 T_0}-\frac{1}{2}\pi^2 PA_1\left(T_2\right)e^{iT_0(\omega+\beta_1)}\\&-\frac{1}{2}\pi^2 PA_2\left(T_2\right)e^{iT_0(-\beta_2+\omega)}-\frac{1}{2}\pi^2 PA_1\left(T_2\right)e^{-iT_0(\omega-\beta_1)}-\frac{1}{2}\pi^2 PA_2\left(T_2\right)e^{-iT_0(\beta_2+\omega)}+NST\end{aligned} \tag{22}$$

where NST stands for non-secular terms.

4 COMBINATION RESONANCE

Now, combination resonance of forward and backward modes is considered. By introducing the detuning parameters σ for describing the nearness of ω to $\beta_1+\beta_2$ it can be written [24]:

$$\omega=\beta_1+\beta_2+\varepsilon^2\sigma \tag{23}$$

Substituting (23) into (22) and separating secular terms, the modulation equations are obtained:

$$\left(\Gamma_1 A_1'(T_2)-\mu_1 A_1(T_2)\right)i-\alpha\pi^4\left(\overline{A}_1(T_2)A_1(T_2)^2+2\overline{A}_2(T_2)A_2(T_2)A_1(T_2)\right)-\Lambda A_2(T_2)e^{i\sigma_2 T_2}=0 \tag{24}$$

$$\left(\Gamma_2 A_2'(T_2)+\mu_2 A_2(T_2)\right)i-\alpha\pi^4\left(\overline{A}_2(T_2)A_2(T_2)^2+2\overline{A}_1(T_2)A_1(T_2)A_2(T_2)\right)-\Lambda A_1(T_2)e^{-i\sigma_2 T_2}=0 \tag{25}$$

where prime ($'$) indicates the derivative with respect to T_2 and μ_k ,Γ_k $(k=1,2)$ and Λ are defined in Appendix A.

We introduce the polar transformation as follows [23]:

$$A_k(T_2)=a_k(T_2)e^{i\theta_k(T_2)},\quad k=1,2 \tag{26}$$

Putting (26) into (24) and (25), separating real and imaginary parts, the following equations are obtained:

$$\Gamma_1 a_1'(T_2)=\mu_1 a_1(T_2)+\Lambda a_2(T_2)\sin\left(\theta_2(T_2)-\theta_1(T_2)+\sigma T_2\right) \tag{27}$$

$$\Gamma_1 a_1(T_2)\theta_1'(T_2)=-\alpha\pi^4\left[a_1^3(T_2)+2a_1(T_2)a_2^2(T_2)\right]-\Lambda a_2(T_2)\cos\left(\theta_2(T_2)-\theta_1(T_2)+\sigma T_2\right) \tag{28}$$

$$\Gamma_2 a_2'(T_2)=-\mu_2 a_2(T_2)-\Lambda a_1(T_2)\sin\left(\theta_2(T_2)-\theta_1(T_2)+\sigma T_2\right) \tag{29}$$

$$\Gamma_2 a_2(T_2)\theta_2'(T_2)=-\alpha\pi^4\left[a_2^3(T_2)+2a_2(T_2)a_1^2(T_2)\right]-\Lambda a_1(T_2)\cos\left(\theta_2(T_2)-\theta_1(T_2)+\sigma T_2\right) \tag{30}$$

Following transformation is used to transform above non autonomous system to autonomous one [24]:

$$\begin{aligned}&\psi(T_2)=\theta_2(T_2)-\theta_1(T_2)+\sigma T_2\\&\psi'(T_2)=\theta_2'(T_2)-\theta_1'(T_2)+\sigma\end{aligned} \tag{31}$$

Multiplying (30) by $\Gamma_1 a_1(T_2)$ and (28) by $\Gamma_2 a_2(T_2)$, subtracting the results, using (31) the following equation is obtained:

$$\begin{aligned}&\Gamma_1\Gamma_2 a_1(T_2)a_2(T_2)\psi'(T_2)=\Gamma_1\Gamma_2 a_1(T_2)a_2(T_2)\sigma+\alpha\pi^4\left[\Gamma_2 a_2(T_2)a_1^3(T_2)+2\Gamma_2 a_1(T_2)a_2^3(T_2)\right]\\&-\alpha\pi^4\left[\Gamma_1 a_1(T_2)a_2^3(T_2)+2\Gamma_1 a_2(T_2)a_1^3(T_2)\right]+\Lambda\left[\Gamma_2 a_2^2(T_2)-\Gamma_1 a_1^2(T_2)\right]\cos\left(\psi(T_2)\right)\end{aligned} \tag{32}$$

This is a modulation equation governs the behavior of slow time scale of the motion. For steady state response of the rotor, a' and ψ' are zero. Hence (27), (29) and (32) can be written in terms of ψ as follows:

$$\mu_1 a_1=-\Lambda a_2\sin\psi \tag{33}$$

$$-\mu_2 a_2 = \Lambda a_1 \sin\psi \tag{34}$$

$$\Gamma_1\Gamma_2 a_1 a_2 \sigma + \alpha\pi^4\left[\Gamma_2 a_2 a_1^3 + 2\Gamma_2 a_1 a_2^3 - \Gamma_1 a_1 a_2^3 - 2\Gamma_1 a_2 a_1^3\right] = \Lambda\left[\Gamma_1 a_1^2 - \Gamma_2 a_2^2\right]\cos(\psi) \tag{35}$$

Multiplying (33) by a_2 and (34) by a_1, and dividing the results, the following relation between a_1 and a_2 is obtained:

$$a_2 = \chi a_1 , \quad \chi = \sqrt{\frac{\beta_1}{\beta_2}} \tag{36}$$

Eq. (36) shows the relation between forward and backward amplitudes. In the next section, it will be shown that χ is nearly one. Now, multiplying (33) by $\Gamma_2 a_2(T_2)$ and (34) by $\Gamma_1 a_1(T_2)$, and adding the results, the following equation is achieved:

$$a_1 a_2\left(\Gamma_2\mu_1 - \Gamma_1\mu_2\right) = \Lambda\left(\Gamma_1 a_1^2 - \Gamma_2 a_2^2\right)\sin\psi \tag{37}$$

It can be shown that $\Gamma_2 = -\Gamma_1$. From this fact and by using (36), we can write (37) and (35) as:

$$-\Theta\mu = \sin\psi \tag{38}$$

$$\Xi\sigma - \Pi\alpha a_1^2 = \cos\psi \tag{39}$$

where

$$\Theta = \frac{\chi}{\Lambda\left(\chi^2+1\right)},\ \Xi = \frac{\Gamma_2\chi}{\Lambda\left(\chi^2+1\right)},\ \Pi = \frac{3\pi^2\chi}{\Lambda},\ \mu = \mu_1 + \mu_2 \tag{40}$$

Squaring (38) and (39), adding the results, the frequency response equation is found as:

$$a_1^2 = \frac{\Xi}{\Pi}\frac{\sigma}{\alpha} \pm \frac{1}{\Pi\alpha}\left[1 - \Theta^2\mu^2\right]^{0.5} \tag{41}$$

Eqs. (41) and (36) explicitly compute forward and backward amplitudes of the motion in terms of system parameters in the case of combination resonance.

4 NUMERICAL EXAMPLES

In this section, numerical examples are considered to examine the behavior of system. All the parameters which are used in this section are non-dimensional parameters. In all cases $\Omega = 10.25,\ I_2 = 0.000625,\ \alpha = 0.0003,\ f = 0.0565$ except where other values are mentioned.

Fig. 2 shows the frequency response curves for forward and backward amplitudes, i.e. a_1 and a_2. One can obtain from (36) that χ is almost one so the amounts of both amplitudes are nearly equal. Stationary points of Eq. (41) may be stable or unstable. One can use Jacobian matrix of (38) and (39) to show the stability of these points [24]. In Fig. 2 solid lines and dotted lines are used to indicate stable and unstable branches. It is obvious from Fig. 2 that jump phenomenon is possible. The numerical integration of discretized equations of motion has been used to validate the result of analytical solution. It is seen from Fig. 2 that both solutions are in good agreement. This graph

also shows hardening type because the curves are bent toward the side of increasing exciting frequency. For further discussion about details of Fig. 2 one can refer to [24].

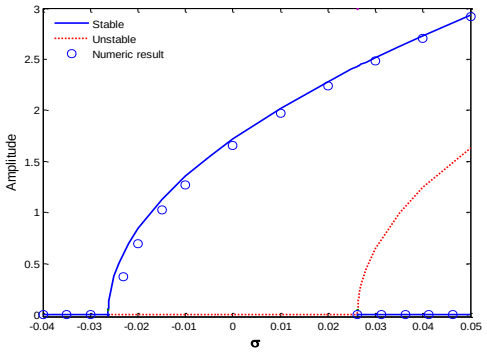

Fig.2
Frequency response curves of a_1 and a_2 for $\mu_e = 0.01$ and $P = 0.056$. $a_1 \approx a_2$.

Fig. 3(a) shows time history of the system when the response reaches to steady state. The Fourier transform of this graph has been indicated in Fig. 3(b). The graph shows amplitudes of forward and backward frequencies. It is obvious that both forward and backward amplitudes are equal and this is in agreement with previous result from (36).

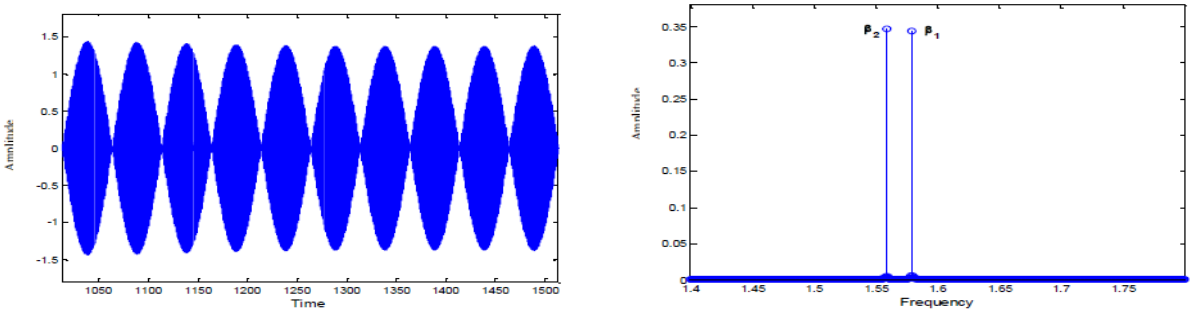

(a) (b)

Fig.3
a) Time history and b) Fourier transformation for $\mu_e = 0.01$, $P = 0.056$ and $\sigma = -0.02$.

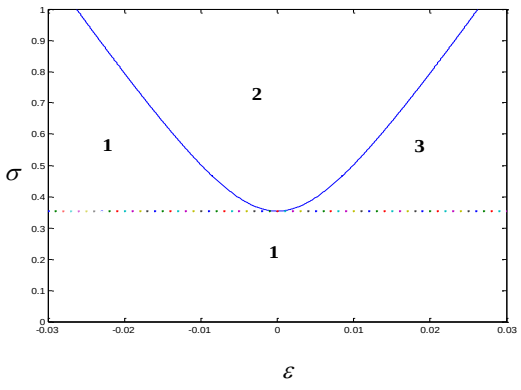

Fig.4
The various regions in parameter space for $\mu_e = 0.01, P = 0.056$.

Here, the effect of damping on the system response is discussed. To do this, one can rewrite (41) as [24]:

$$a_1^2 = \frac{\Xi}{\Pi}\frac{\hat{\sigma}}{\hat{\alpha}} \pm \frac{1}{\Pi\hat{\alpha}}\left[\varepsilon^2 - \Theta^2\hat{\mu}^2\right]^{0.5} \tag{42}$$

where $\hat{\mu}=\varepsilon\mu$, $\hat{\alpha}=\varepsilon\alpha$ and $\hat{\sigma}=\varepsilon\sigma$. It is obvious that right hand side of (42) should be positive and as a result the following relations are obtained:

$$\hat{\sigma}=\pm\frac{1}{\Xi}\left(\varepsilon^2-\Theta^2\hat{\mu}^2\right)^{0.5}$$
$$\varepsilon=\pm\Theta\mu \tag{43}$$

Fig. 4 shows that the $\varepsilon\sigma$-plane (parametric plane) is divided into three regions by the curves governed by (43). It can be seen that below the line $\varepsilon=-\Theta\hat{\mu}$, the response always decays and it shows the effect of damping in the system. Some authors [24, 25] showed that external damping may have a destabilizing effect on combination resonances in linear systems.

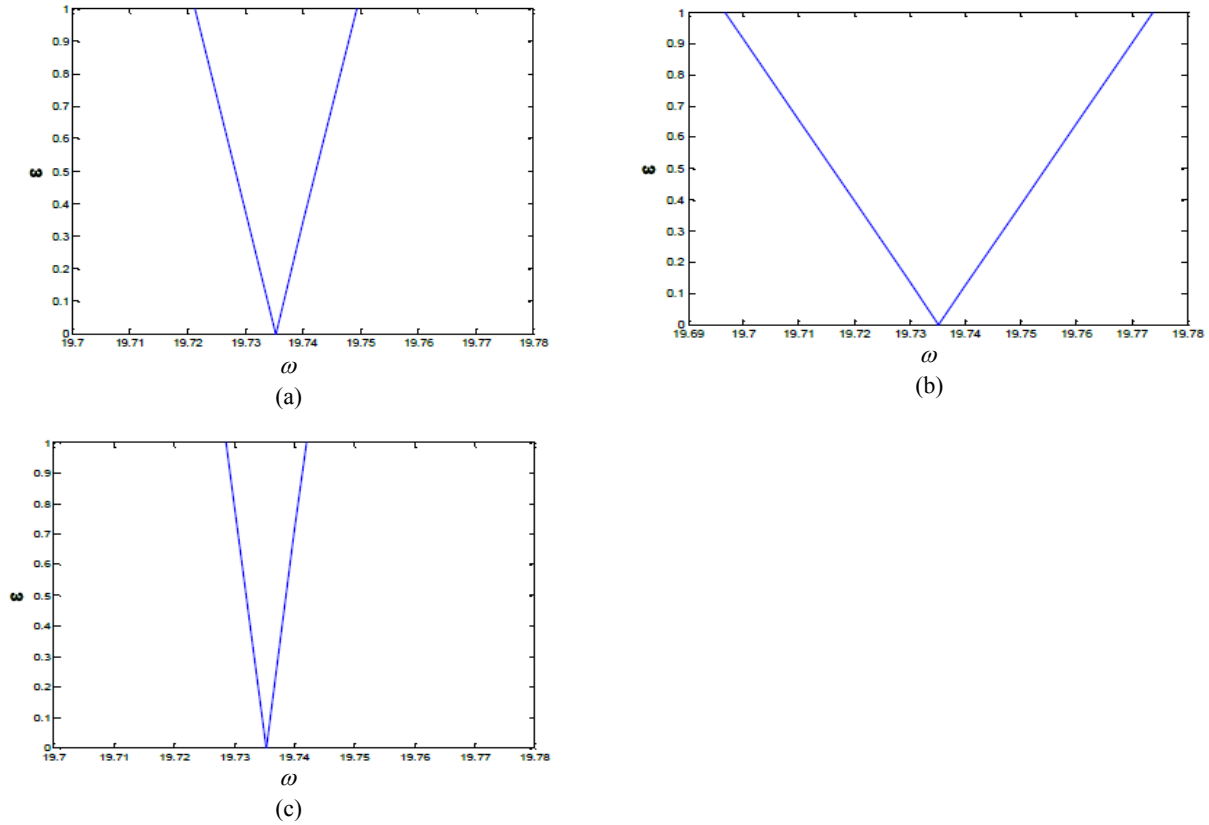

Fig.5
Stability regions of linear system for $P=0.056$ when a) $\mu_e=0$, b) $\mu_e=0.03$, c) $\mu_e=0.053$.

The possibility of this effect is examined here by neglecting nonlinear terms in (24) and (25) and we put the following equation in them:

$$A_1(T_2)=a_1(T_2)e^{-i\lambda T_2},\quad A_2(T_2)=a_2(T_2)e^{-i(\lambda+\sigma)T_2} \tag{44}$$

with regard to reference [24], and noting that $\omega=\beta_1+\beta_2+\varepsilon\sigma$, one can obtain stability boundaries of linear system as follows:

$$\varepsilon=\pm\frac{\Gamma_2\left[\omega-\left(\beta_1+\beta_2\right)\right]}{\left(\mu_2+\mu_1\right)\left[\Lambda^2\left(\mu_1\mu_2\right)^{-2}-1\right]^{0.5}} \tag{45}$$

In absence of damping, Eq. (45) reduces to $\varepsilon = \pm \dfrac{\omega - (\beta_1 + \beta_2)}{\Lambda}$. So when damping is present in system and since in general case $\mu_1 \neq \mu_2$, the external damping is destabilizing if:

$$\Lambda^2 < (\mu_2 + \mu_1)^2 \left(\Lambda^2 (\mu_1 \mu_2)^{-2} - 1 \right) \tag{46}$$

This relation is the same with the result in reference [24].

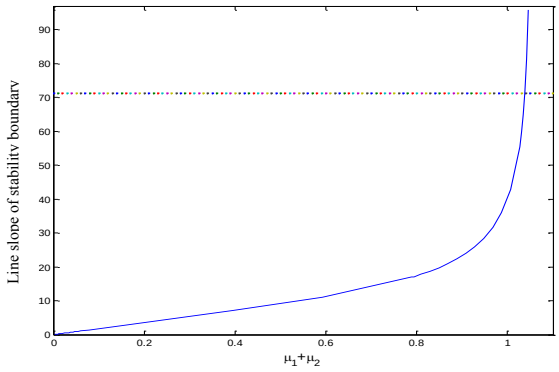

Fig.6
Variation of line slope corresponding to instability boundaries with respect to damping.

Fig. 5 shows stability boundaries of the linear system in three cases. In case (a), there is no damping in system. Case (b) indicates destabilizing effect of external damping when condition (46) is satisfied and in case (c), the stabilizing effect of damping has been shown. The change of line slope with respect to $\mu_1 + \mu_2$ has been indicated in Fig. 6. In this figure, the slope of line is 71.22 for zero damping. A horizontal line is drawn to indicate the separation of stable region from unstable region according to variation of damping. In other words, below the horizontal line is the region where the line slope of the linear system with damping is less than a same system with no damping and as a result, damping has destabilizing effect. When the amount of horizontal line reaches to 1.038 (i.e. $\mu_1 + \mu_2 = 1.038$), damping stabilizes the system.

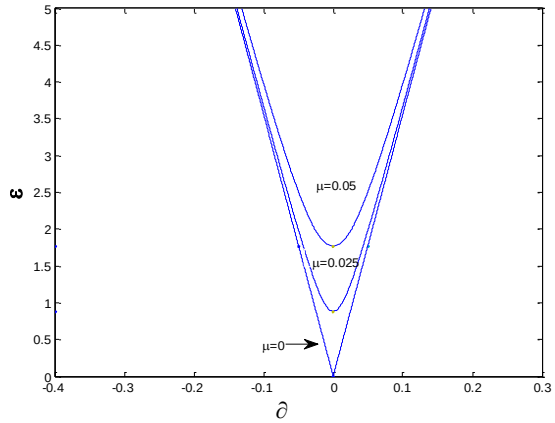

Fig.7
Effect of damping in parametric space for $P = 0.056$.

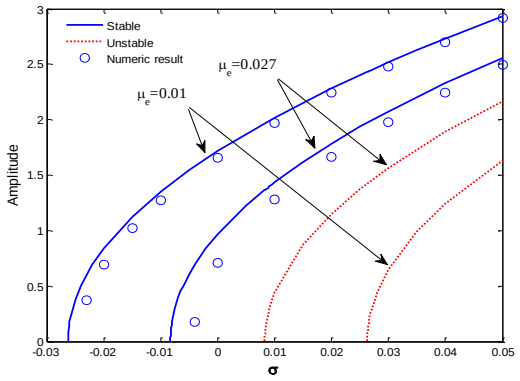

Fig.8
Frequency response curves of a_1 and a_2 for different μ_e when $P = 0.056$.

According to Fig. 6, the variation of line slope with respect to damping is linear when $\mu_1 + \mu_2 < 0.8$. From this point, the variation of line slope becomes very rapid and with a small variation in $\mu_1 + \mu_2$, a big variation in slope of the line occurs. Now, we turn our attention to nonlinear case. From (43) and Fig. 4, it is obvious that external damping in nonlinear system can increase region 1 and reduce region 2 as indicated in Figs. 7 and 8. So, one can say that unusual effect of external damping on combination resonances of linear system is not valid in nonlinear system with same conditions. In other words, considering the nonlinearity is necessary in computation of unstable region. The external damping has great influence on nonlinear system by reducing region 2. If damping exceeds some specific value, then the response of system always decays.

In Fig. 8, the graph has been plotted for three values of damping. By increasing damping coefficient, the distance between stable and unstable branches reduces until two branches completely disappear.

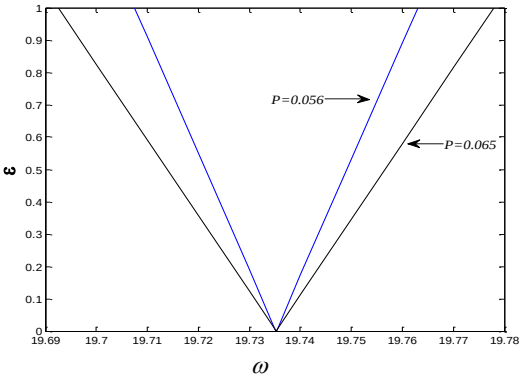

Fig.9
Stability regions of linear system for different periodic axial load when $\mu_e = 0.05$.

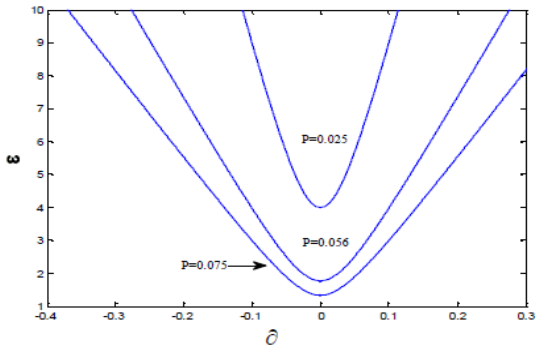

Fig.10
Effect of periodic axial load in parametric space for $\mu_e = 0.05$.

Now, the influence of axial load on the behavior of response is considered in both linear and nonlinear cases. Fig. 9 shows stability boundaries of linear system. With increasing dynamic part of axial load, the region of instability grows. It is clear from (45) that increasing of P decreases the slope of graph and hence the instable zone increases.

Although, in the nonlinear system, the same result is obtained but, nonlinearity limits the amplitude of vibration and as a result, region 2 in Fig. 10 does not indicate unstable response. With increasing P, the graph of Fig. 10 becomes wider.

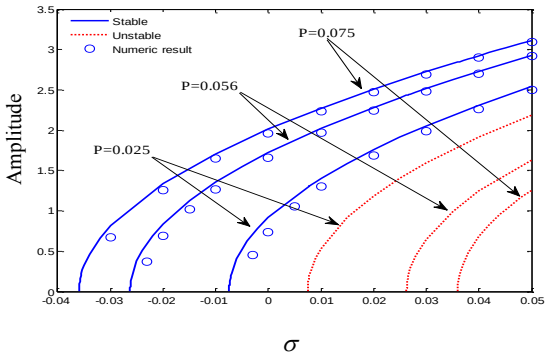

Fig.11
Frequency response curves of a_1 and a_2 for different P when $\mu_e = 0.01$.

Fig. 11 shows frequency response curves for different amount of dynamic axial load. For a constant frequency, with increasing P, the response grows. It is also seen from Fig. 11 that the distance between stable and unstable branches changes with variation of P.

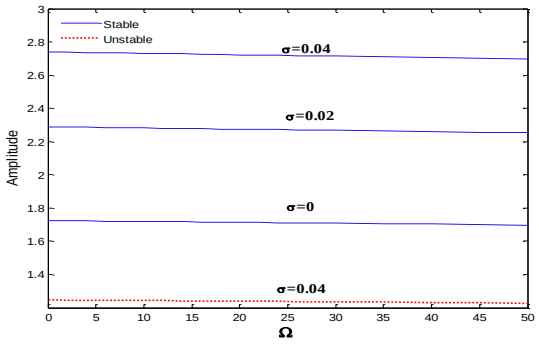

Fig.12
Variation of amplitude a_1 and a_2 with respect to Ω for $\mu_e = 0.01, P = 0.056$.

It should be noted that to avoid confusion, the solutions with zero amplitude have not been shown in Figs. 8 and (11). Figs. 12 and 13 show the amplitude of response with respect to spin and rotary inertia for three different frequencies. In both cases, the amplitude of vibration almost does not vary with variation of Ω and I_2. In fact, variation in spin or rotary inertia just changes the amount of natural frequencies and has not any influence on amplitude. One can test that in linear case, the width of unstable region does not change with increasing or decreasing of spin or rotary inertia.

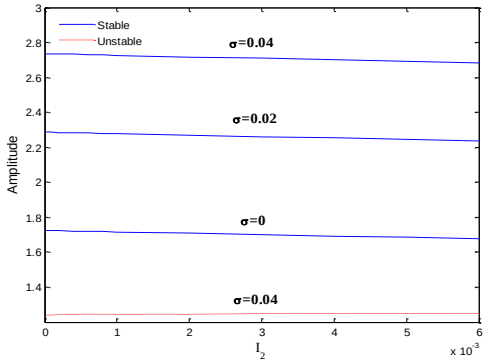

Fig.13
Variation of amplitude a_1 and a_2 with respect to I_2 for $\mu_e = 0.01, P = 0.056$.

5 CONCLUSIONS

In this paper, the dynamic behavior of a balanced nonlinear rotating shaft under a periodic axial load with presence of external damping was investigated. Rotary inertia and gyroscopic effects were included but shear deformation was neglected. To analyze the system, multiple scales method was used to derive a set of four first–order nonlinear ordinary differential equations describing the modulation of amplitudes and phases of forward and backward whirling motion. These equations were simplified to one algebraic nonlinear equation by some mathematical operations. The stability of system was ascertained by determining the sign of eigenvalues of the corresponding Jacobian matrix. The type of excitation was combination resonance due to periodic axial load. The effect of various parameters on system response was discussed and the influence of external damping on linear and nonlinear system was clarified.

The most important results of the paper can be expressed as:

- Trivial and nontrivial solutions coexist.
- External damping on combination resonances of linear system may have destabilizing effect but in nonlinear system, it always reduces the amplitude and from a specific amount of damping coefficient, the response decays to zero for all frequencies.
- By increasing periodic axial load, the distance between stable and unstable branches getting wider.
- Variation in spin and rotary inertia does not mainly change the amplitude.
- The results of numerical simulation and the perturbation solutions are in good agreement.

APPENDIX A

$$\Gamma_1 = 2I_2\Omega\pi^2 - 2I_2\pi^2\beta_1 - 2\beta_1,$$

$$\Gamma_2 = 2\beta_2 + 2I_2\pi^2\beta_2 + 2I_2\Omega\pi^2,$$

$$\mu_1 = \mu_e\beta_1, \mu_2 = \mu_e\beta_2,$$

$$\Lambda = \frac{1}{2}\pi^2 P$$

REFERENCES

[1] Chen L. W., Ku D. M., 1990, Dynamic stability analysis of a rotating shaft by the finite element method, *Journal of Sound and Vibration* **143**(1): 143-151.

[2] Lee H. P., Tan T. H., Leng G. S. B., 1997, Dynamic stability of spinning timoshenko shafts with a time-dependent spin rate, *Journal of Sound and Vibration* **199**(3): 401-415.

[3] Sheu H.C., Chen L.W., 2000, A lumped mass model for parametric instability analysis of cantilever shaft–disk systems, *Journal of Sound and Vibration* **234**(2): 331-348.

[4] Pei Y.C., 2009, Stability boundaries of a spinning rotor with parametrically excited gyroscopic system, *European Journal of Mechanics - A/Solids* **28**(4): 891-896.

[5] Bartylla D., 2012, Stability investigation of rotors with periodic axial force, *Mechanism and Machine Theory* **58**: 13-19.

[6] Mailybaev A. A., Seyranian A. P., 2013, Instability of a general rotating system with small axial asymmetry and damping, *Journal of Sound and Vibration* **332**(2): 346-360.

[7] Mailybaev A. A., Spelsberg-Korspeter G., 2015, Combined effect of spatially fixed and rotating asymmetries on stability of a rotor, *Journal of Sound and Vibration* **336**: 227-239.

[8] Bolotin V.V., 1964, *The Dynamic Stability of Elastic System* , Holden-day, Sanfransico, CA.

[9] Yamamoto T., Ishida Y., Aizawa K., 1979, On the subharmonic oscillations of unsymmetrical shafts, *Bulletin of JSME* **22**(164): 164-173.

[10] Yamamoto T., Ishida Y., Ikeda T., 1981, Summed-and-differential harmonic oscillations of an unsymmetrical shaft, *Bulletin of JSME* **24**(187): 183-191.

[11] Yamamoto T., Ishida Y., Ikeda T., Yamada M.,1981, Subharmonic and summed-and-differential harmonic oscillations of an unsymmetrical rotor, *Bulletin of JSME* **24**(187): 192-199.

[12] Yamamoto T., Ishida Y., Ikeda T., Suzuki H., 1982, Super-summed-and-differential harmonic oscillations of an unsymmetrical shaft and an unsymmetrical rotor, *Bulletin of JSME* **25**(200): 257-264.

[13] Yamamoto T., Ishida Y., Ikeda T., Yamamoto M., 1982, Nonlinear forced oscillations of a rotating shaft carrying an unsymmetrical rotor at the major critical speed, *Bulletin of JSME* **25**(210): 1969-1976.

[14] Yamamoto T., Ishida Y., Ikeda T., 1983,Vibrations of a rotating shaft with rotating nonlinear restoring forces at the major critical speed, *Transactions of the Japan Society of Mechanical Engineers Series C* **49**(448): 2133-2140.

[15] Ishida Y., Ikeda T., Yamamoto T., 1986, Effects of nonlinear spring characteristics on the dynamic unstable region of an unsymmetrical rotor, *Bulletin of JSME* **29**(247): 200-207.

[16] Ishida Y., Liu J., Inoue T., Suzuki A., 2008,Vibrations of an asymmetrical shaft with gravity and nonlinear spring characteristics (Isolated Resonances and Internal Resonances), *Journal of Vibration and Acoustics* **130**: 041004.

[17] Shahgholi M., Khadem S. E., 2012, Primary and parametric resonances of asymmetrical rotating shafts with stretching nonlinearity, *Mechanism and Machine Theory* **51**: 131-144.

[18] Shahgholi M., Khadem S.E., Bab S., 2015, Nonlinear vibration analysis of a spinning shaft with multi-disks, *Meccanica* **50**: 2293-2307.

[19] Ghorbanpour Arani A., Haghparast E., Amir S., 2012, Analytical solution for electro-mechanical behavior of piezoelectric rotating shaft reinforced by BNNTs under nonaxisymmetric internal pressure, *Journal of Solid Mechanics* **4**: 339-354.

[20] Hosseini S. A. A., Zamanian M., 2013, Multiple scales solution for free vibrations of a rotating shaft with stretching nonlinearity, *Scientia Iranica* **20**(1): 131-140.

[21] Ishida Y., Nagasaka I., Inoue T., Lee S., 1996, Forced oscillations of a vertical continuous rotor with geometric nonlinearity, *Nonlinear Dynamics* **11**(2): 107-120.

[22] Nayfeh A.H., Pai P.F., 2004, *Linear and Nonlinear Structural Mechanics,* Wiley, New York.

[23] Nayfeh A. H.,1981, *Introduction to Perturbation Techniques*, Wiley, New York.

[24] Nayfeh A. H., Mook D. T., 1979, *Nonlinear Oscillations*, Wiley, New York.

[25] Valeev K. G., 1963, On the danger of combination resonances, *Journal of Applied Mathematics and Mechanics* **27**(6): 1745-1759.